AJNR

High-Resolution Vascular Imaging of the Rat Spine Using Liposomal Blood Pool MR Agent

K.B. Ghaghada, K.H.J. Bockhorst, S. Mukundan, Jr, A.V. Annapragada and P.A. Narayana

AJNR Am J Neuroradiol 2007, 28 (1) 48-53
http://www.ajnr.org/content/28/1/48

ORIGINAL RESEARCH

K.B. Ghaghada
K.H.J. Bockhorst
S. Mukundan, Jr
A.V. Annapragada
P.A. Narayana

High-Resolution Vascular Imaging of the Rat Spine Using Liposomal Blood Pool MR Agent

BACKGROUND AND PURPOSE: High-resolution, vascular MR imaging of the spine region in small animals poses several challenges. The small anatomic features, extravascular diffusion, and low signal-to-noise ratio limit the use of conventional contrast agents. We hypothesize that a long-circulating, intravascular liposomal-encapsulated MR contrast agent (liposomal-Gd) would facilitate visualization of small anatomic features of the perispinal vasculature not visible with conventional contrast agent (gadolinium-diethylene-triaminepentaacetic acid [Gd-DTPA]).

METHODS: In this study, high-resolution MR angiography of the spine region was performed in a rat model using a liposomal-Gd, which is known to remain within the blood pool for an extended period. The imaging characteristics of this agent were compared with those of a conventional contrast agent, Gd-DTPA.

RESULTS: The liposomal-Gd enabled acquisition of high quality angiograms with high signal-to-noise ratio. Several important vascular features, such as radicular arteries, posterior spinal vein, and epidural venous plexus were visualized in the angiograms obtained with the liposomal agent. The MR angiograms obtained with conventional Gd-DTPA did not demonstrate these vessels clearly because of marked extravascular soft-tissue enhancement that obscured the vasculature.

CONCLUSIONS: This study demonstrates the potential benefit of long-circulating liposomal-Gd as a MR contrast agent for high-resolution vascular imaging applications.

Compromised vasculature is implicated in a number of spine pathologies.[1,2] Moreover, demonstration of perispinal vasculature is important for presurgical planning.[3] Imaging of mid-size and large vascular structures is aided by the use of exogenous contrast agents that are typically imaged on first pass through the arterial circuit by using a fast acquisition, which is referred to as contrast-enhanced magnetic resonance angiography (CE-MRA).[4-6] Unfortunately, the role of CE-MRA has been limited in the evaluation of smaller vessels because of the long scan times required and the resulting venous contamination.

Rodent models are commonly used to study spinal cord pathologies, particularly spinal cord injury.[7-12] MR angiography (MRA) of the spine in rodents, however, presents unique challenges because of the small size of the blood vessels (approximately 100–300 μm). Visualization of these vessels with high signal-to-noise ratio (SNR) requires significant signal intensity averaging and involves relatively long acquisition times.

In the present work, we report the use of gadolinium-encapsulated long-circulating liposomes (liposomal-Gd) for high-resolution MR imaging of the rat spinal vasculature. Although there is some variability in the literature, we define high-resolution MRA as imaging at spatial resolution of approximately 100 μm and use it as such in the present context. Long-circulating liposomes are nanoparticles (~100 nm) bearing hydrophilic polyethylene glycol (PEG) chains on their external surface. The PEG coating prevents opsonization and prolongs circulation half-life to around 18 hours.[13] The long intravascular half-life of this agent results in stable levels of contrast agent within the blood pool for many hours, thus enabling a longer image acquisition time window. Beyond this, there is relative lack of enhancement of the adjacent extravascular tissue that results in a high contrast-to-noise ratio. We therefore hypothesize that a long-circulating, intravascular liposomal-encapsulated MR contrast agent (liposomal-Gd) would facilitate visualization of small anatomic features of the perispinal vasculature in a rat model not visible with conventional contrast agent (Gd-DTPA).

Received January 27, 2006; accepted after revision March 14.

From the Department of Chemical Engineering (K.B.G.), University of Houston, Tex; School of Health Information Sciences (K.B.G., A.V.A.), University of Texas Health Science Center, Tex; Department of Radiology (K.H.J.B., P.A.N.), University of Texas-Houston Medical School, Tex; Department of Radiology (S.M.), Duke University Medical Center, NC; Department of Biomedical Engineering (S.M.), Duke University, NC.

Partial support for these studies was provided by National Science Foundation grant BES 0201891 (A.V.A.) National Institutes of Health grant R01-NS30821 (P.A.N.), Chandran Family Foundation (S.M.), and the American Roentgen Ray Society (S.M.).

Address correspondence to Ananth V. Annapragada, PhD, 7000 Fannin St, Suite 600, Houston, TX 77030; e-mail: ananth.annapragada@uth.tmc.edu

Methods

Liposomal-Gd Preparation

Liposomal-Gd was prepared by modification of methods described previously.[14,15] In brief, a lipid mixture consisting of 1,2-dipalmitoyl-*sn*-glycero-3-phosphocholine (Genzyme, Cambridge, Mass), cholesterol (Sigma, St Louis, Mo) and 1,2-distearoyl-*sn*-glycero-3-phosphoethanolamine-*N*-[methoxy(poly(ethylene glycol))-2000] (Genzyme) in the ratio 55:40:5 was dissolved in ethanol at 60°C. The ethanol solution was then hydrated with 0.5 mol/L gadodiamide (Omniscan–Gd-DTPA BMA; GE Healthcare, Chalfont St. Giles, UK) solution and stirred for 1 hour at 60°C. The resulting liposomal solution was sequentially extruded at 60°C on Lipex Thermoline extruder (Northern Lipids, Vancouver, BC, Canada) with 3 passes through 0.4-μm Nuclepore membrane (Waterman, Newton, Mass), 5 passes through a 0.2-μm Nuclepore membrane, and 8 passes through a 0.1-μm Nuclepore membrane. The external phase was then cleaned, and the liposomes simultaneously concentrated by diafiltration using MicroKros modules (Spectrum Laboratories, Ca) of 50-nm cutoff. The size of the resultant liposomal formulations obtained was determined by dynamic light scattering (DLS) using a BI-9000AT Digital Autocorrelator (Brookhaven Instruments, Holtsville, NY), a BI-

200SM goniometer (JDS Uniphase, San Jose, Calif), and a Hamamatsu photomultiplier (supplied by Brookhaven, Long Island, NY). The resultant size of liposomes in the formulation as determined using DLS was 105 nm with a polydispersity index of 0.107.

The concentration of gadolinium in the liposomal-Gd formulation was determined by inductively coupled plasma atomic emission spectroscopy. The average concentration of Gd in the formulation was found to be 90 mmol/L. To determine the in vitro molar T1 relaxivity of the liposomal-Gd formulation, samples with Gd concentrations ranging between 0.5 and 2 mmol/L (4 samples) were prepared by diluting the original liposomal formulation with phosphate buffered saline. The T1 relaxation times of the samples were then determined on a 7T scanner (BioSpec 70/30 USR; Bruker BioSpin, Karlsruhe, Germany) using a multispin multiecho sequence with the following parameters: TE was 9 ms, and TR varied from 40 to 16,000 ms. A plot of the T1 relaxation rates versus Gd concentrations yielded a straight line with the slope as the in vitro T1 relaxivity of the formulation, which was found to be 0.8 $(mM \cdot s)^{-1}$.

Animal Preparation

All animal studies were performed under a protocol approved by the Animal Welfare Committee of the University of Texas-Houston Health Science Center. Five Sprague-Dawley rats weighing between 350 and 390 g were used in this study. After spontaneous inhalation of 4% isoflurane, the animal was intubated and maintained under anesthesia by ventilating a mixture of 2% isoflurane, 30% oxygen, and air with a vaporizer (Isotec3, Ohmeda, UK) and administered through a Harvard rodent ventilator (Harvard Apparatus, South Natick, Mass). The left jugular vein was cannulated for intravenous delivery of the contrast agent, as described previously.[16] A rectangular coil (11 × 35 mm) was implanted in the back of the animal and centered at the T7 level and inductively coupled to an external surface coil (30 × 40 mm) for improved image quality.[17] The animal was placed in the supine position over the external coil on a custom-built Plexiglas sled and the entire assembly was inserted into the bore of the magnet. The body temperature was maintained at 37°C by circulating warm water through the animal bed throughout the MR imaging scan.

MR Imaging Protocol

All MR studies were performed on a 7T scanner (Bruker BioSpec 70/30 USR), using a 116-mm shielded gradient insert that is capable of producing a maximum gradient amplitude of 400 mT/m with 80-μs rise time. After the acquisition of an orthogonal scout image for animal positioning, anatomic images were obtained using a T1-weighted spin-echo sequence with TE/TR = 10.4/500 ms, 26-mm field of view, and 20 interleaved contiguous axial sections, each 1-mm thick. Preliminary scans were performed for optimizing the scan parameters (echo time, repetition time, and flip angle) for MRA, and the same parameters were used for all the subsequent scans.

Standard Resolution Studies

Precontrast, post-lipsonal-Gd, and post–Gd-DTPA images were acquired as described below. Separate animals were used to evaluate Gd-DTPA and liposomal-Gd to avoid confounding issues that could result from interactions between the 2 contrast agents. The images were acquired using a flow-compensated, fast 3D gradient-echo (GE) sequence with the following parameters: TR/TE, 18.3/2.8 ms; flip angle, 30°; image matrix, 128 × 128 × 64; FOV, 41 × 28 × 25 mm; bandwidth, 200 kHz. The data were acquired with 1 signal intensity average, thus resulting in a scan time of 2.5 minutes. Signal intensity from the surrounding tissue was reduced by incorporating a 1-ms long magnetization transfer pulse with a frequency offset of 1500 Hz. For the Gd-DTPA study, precontrast images were acquired followed by administration of Gd-DTPA at a dose of 0.1 mmol/kg. The data acquisition for post-Gd-DTPA images was started immediately, and subsequent images were acquired over the next 30 minutes. For the liposomal-Gd study, precontrast images were acquired followed by administration of liposomal-Gd at a dose of 0.1 mmol/kg. Post-liposomal-Gd images were acquired 30 minutes after liposome administration. Images for MRA were acquired without cardiac or respiratory gating. Maximum intensity projections (MIP) (generated using ParaVision 3.0.2 software [Bruker BioSpin MRI, Billerica, Mass] or NIH Image J software [http://rsb.info.nih.gov/ij/]) were used to visualize the angiograms. Contrast-to-noise ratios (CNRs) were calculated for regions of interest in the aorta, epidural venous plexus, intercostal arteries, and hemiazygous vein (HV). The CNR was calculated by subtracting the average signal intensity in the surrounding tissues from the average signal intensity within the blood vessel and then dividing this difference by the standard deviation of the signal intensity within the background (air).

High-Resolution Studies

A high spatial resolution acquisition was performed after the injection of 0.1 mmol/kg of Gd in the form of liposomal-Gd through the jugular vein using the previously implanted catheter. Imaging was performed using a flow-compensated fast 3D GE sequence with the following parameters: TR/TE, 18.3/2.8 ms; flip angle, 30°; image matrix, 256 × 256 × 256; FOV, 41 × 28 × 25 mm; bandwidth, 200 KHz. A voxel size of 160 × 109 × 98 μm was achieved using the above parameters. The number of signal intensity averages was set to 3. The scan time for 1 signal intensity average was 20 minutes. Signal intensity from the surrounding tissue was reduced by incorporating a 1-ms magnetization transfer pulse with a frequency offset of 1500 Hz. Images for MRA were acquired without cardiac or respiratory gating. MIPs (generated using Paravision 3.0.2 software or NIH Image J software) were used to visualize the angiograms. Using the method described above, CNRs were calculated for regions of interest in the posterior spinal vein, epidural venous plexus, anterior spinal artery, and radicular artery (of Adamkiewicz).

Results

For the standard resolution study, MIP images of the thoracic spinal region in the coronal plane were generated from acquisitions obtained before and after the administration of liposomal-Gd and Gd-DTPA (Fig 1). The descending aorta and some of the intercostal arteries are visible on the precontrast image. The Gd-DTPA postcontrast image shows relatively poor image contrast between the vasculature and the surrounding tissue, as a result of enhancement of the extravascular tissues, presumably because of diffusion of the Gd-DTPA into the extracellular space. The scans acquired over the next 30 minutes showed no improvement in image quality. Conversely, the post–liposomal-Gd images showed clear vessel enhancement and negligible tissue enhancement. Given this good target-to-background contrast, more perispinal vasculature is demonstrable on the post–liposomal-Gd images. In fact, the intravascular enhancement observed is greater for the post–Gd-DTPA study, than for the post–liposomal-Gd study. However, the CNRs Gd-DTPA images were lower than for liposomal-Gd images (Table 1). (Subtle differences in image

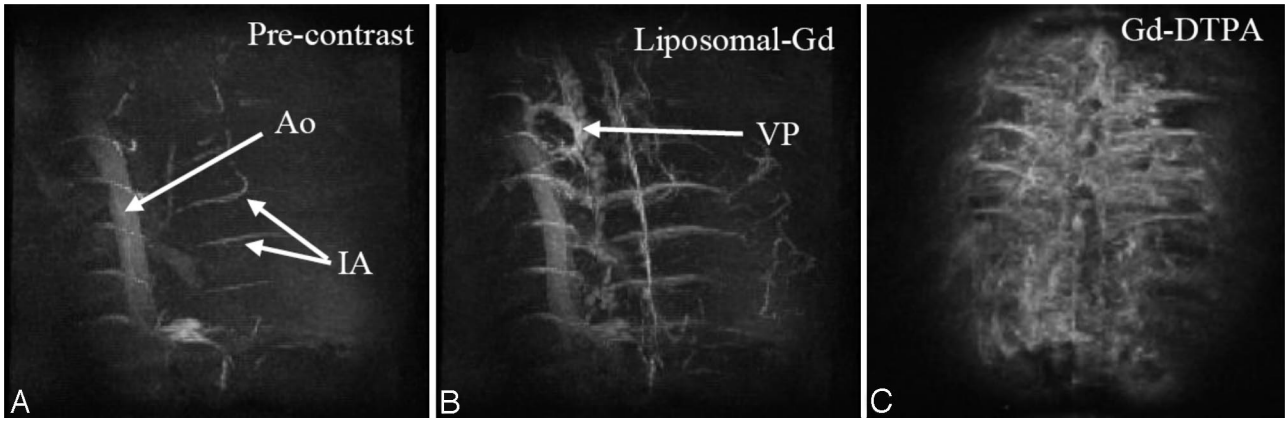

Fig 1. Coronal MIP images of the thoracolumbar spine region acquired precontrast *(A)*, post–liposomal-Gd (*B*), and post–Gd-DTPA (*C*). The images were acquired using the following parameters: TR/TE, 18.3/2.8 ms; flip angle, 30°; image matrix, 128 × 128 × 64; FOV, 41 × 28 × 25 mm; no. of signal intensity average, 1. The total scan time was 2.5 minutes. The descending aorta (Ao), and intercostal arteries (IA) are demonstrated in the precontrast image *(A)*. The epidural venous plexus (VP) and more details about the intercostal arteries are demonstrated in post–liposomal-Gd image *(B)*. The tissue enhancement due to diffusion of Gd-DTPA into the extravasacular space is shown in post-Gd-DTPA image *(C)*. Post–liposomal-Gd and post–Gd-DTPA images were acquired in different animals.

Table 1: Contrast-to-noise ratio (CNR) for anatomic features in standard-resolution images obtained with Gd-DTPA to images obtained with liposomal-Gd

Anatomic Feature	Gd-DTPA	Liposomal-Gd
Epidural venous plexus	8.2	21.0
Intercostal arteries	13.2	22.0
Hemiazygous vein	19.8	36.4
Aorta	8.3	18.2

Note:—Gd-DTPA indicates gadolinium-diethylene-triaminepentaacetic acid; Liposomal-Gd, gadolinium-encapsulated long-circulating liposomes.

orientation in the postcontrast images in Fig 1 are of secondary importance compared with section-selection differences between the datasets, which were acquired using 2 different animals.)

For the high-resolution study, MIP images of the thoracic spinal region were generated in the coronal plane before and after administration of liposomal-Gd (Fig 2). The postcontrast images demonstrate several small blood vessels near the spinal cord, the epidural venous plexus (VP), and the posterior spinal vein (PSV) along the dorsal surface of the spinal cord. The CNRs for liposomal-Gd images were higher than precontrast images (Table 2).

Axial images from the post–liposomal-Gd volume acquisition of the midthoracic spine were also reviewed (Fig 3). The HV is clearly seen in this image. The descending aorta and a section of the inferior vena cava are also visible. In addition, unnamed perforating vessels are identified penetrating the ventral spinal cord (Fig 3*B*, -*D*). Artifacts due to the presence of the surgically implanted radio-frequency coil within the soft tissues of the back are also visible in all the images. The PSV, anterior spinal artery (ASA), and radicular arteries (including presumably the artery of Adamkiewicz with its characteristic hairpin turn) are identified on the MIP images generated in the coronal plane (Fig 4).

Discussion

Small animal vascular MR imaging of the spine poses several challenges. Most of the perispinal vessels are ≤300 μm,[18] and the vessels within the spinal cord are ≤150 μm. Imaging these microvessels necessitates a large image acquisition matrix size

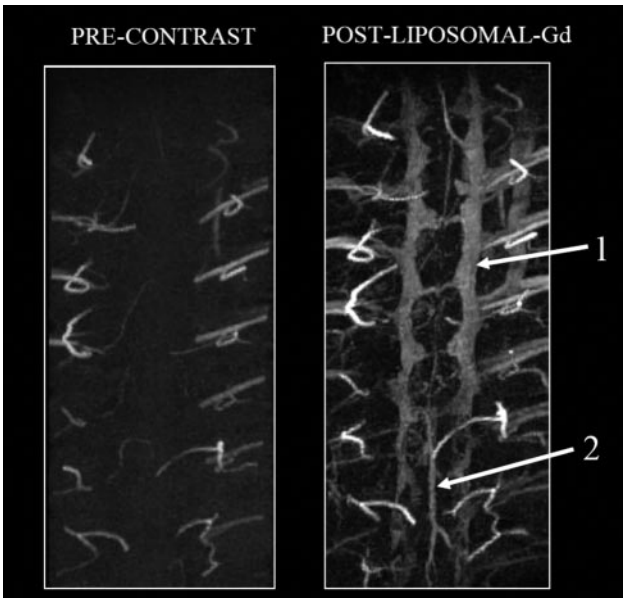

Fig 2. Coronal MIP images of the thoracolumbar spine region acquired before (*left*) and after (*right*) administration of liposomal-Gd. The images were acquired using the following parameters: TR/TE, 18.3/2.8 ms; flip angle, 30°; image matrix, 256 × 256 × 256; FOV, 41 × 28 × 25 mm, no. of signal intensity average, 3. The epidural venous plexus (*1*) and the posterior spinal vein (*2*) are clearly visible in the post–liposomal-Gd image.

Table 2: Contrast-to-noise ratio (CNR) for anatomic features in high-resolution images obtained precontrast and after administration of liposomal-Gd

Anatomic Feature	Precontrast	Liposomal-Gd
Epidural venous plexus	−0.1	6.5
Posterior spinal vein	−0.5	2.3
Anterior spinal artery	1.4	4.1
Radicular artery (of Adamkiewicz)	3.2	6.8

Note:—Liposomal-Gd indicates gadolinium-encapsulated long-circulating liposomes.

(small voxel size) to achieve the required high spatial resolution. Unfortunately, this results in a concomitant reduction in the SNR. To overcome the penalty in SNR imposed by the acquisition matrix, data have to be acquired with several signal intensity averages, which, unfortunately, comes at the cost of longer acquisition times.

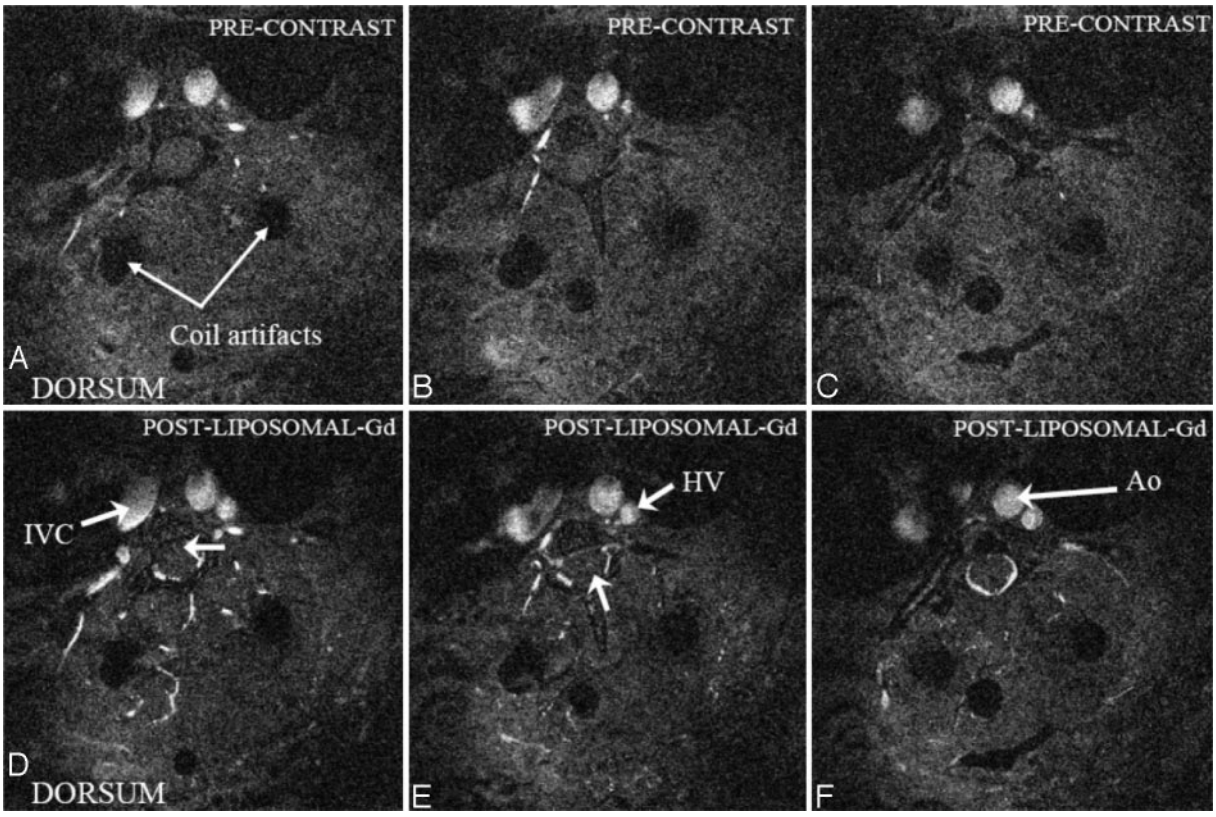

Fig 3. Precontrast (*top row*) and postcontrast (*bottom row*) axial sections at different locations through the thoracolumbar spine region showing several important vascular features (Ao, aorta, IVC, inferior vena cava; HV, hemiazygous vein). Blood vessels penetrating the spinal cord can be visualized in *D* and *E* (*arrow*). The epidural venous plexus is demonstrated in *F*. The artifacts due to the implantation of radio-frequency coil on the dorsal side are also visible. These images are acquired after administration of liposomal-Gd.

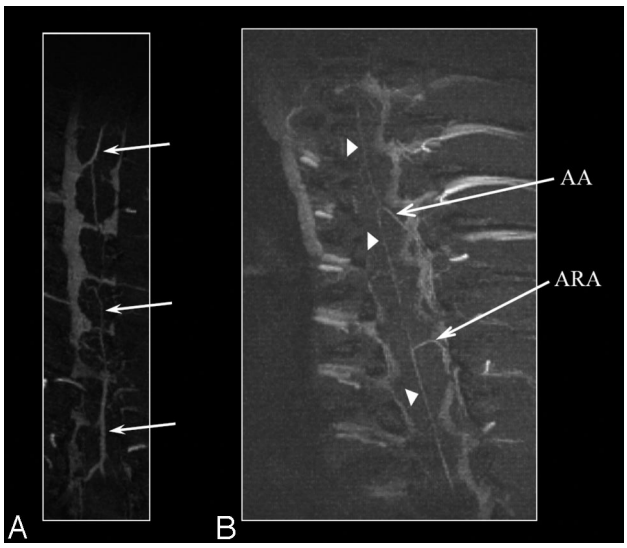

Fig 4. Coronal MIP images of the thoracolumbar spine region obtained with liposomal-Gd. The posterior spinal vein (PSV) is clearly seen in *A* (*arrows*). The anterior spinal artery (*arrowheads*), the artery of Adamkiewicz (AA) and an accessory anterior radicular artery (ARA) can be clearly seen in *B*.

Most studies of rodent spinal vasculature have therefore been based on invasive imaging. Tveten[19,20] investigated the vasculature of the rat spinal region using microangiographic and stereomicroscopic techniques. Koyangi et al[18] have analyzed the rat spinal cord vasculature with scanning electron microscope examination of a vascular corrosion cast. MR imaging techniques have not yet yielded sufficient information on the vasculature. For instance, Bilgen et al[17] studied spinal MRA at 9.4T without the use of any exogenous contrast agent and in conjunction with the time-of-flight technique.[21] Although some of the intercostal arteries were visible, the lack of contrast agent within the vasculature for a sustained interval prevented high-resolution studies and also precluded visualization of intracord vasculature. Yet the promise of high-resolution, noninvasive imaging is alluring and motivates the current work.

An ideal contrast agent for this type of data acquisition (long-duration, large image matrix) should have the following characteristics: the contrast agent must 1) remain confined to the vasculature and 2) maintain a relatively constant concentration (low elimination, dilution, and redistribution during the period of the data acquisition). If the contrast agent exits the intravascular space during the acquisition period, the CE-MRA images are degraded for 2 reasons. First, the relaxation time of blood is increased and the signal intensity from blood is reduced at short TR. Second, the contrast agent diffuses into the surrounding tissue and reduces the relaxation time, resulting in increased signal intensity from the surrounding tissue. As a result, the image contrast between blood vessels and the surrounding tissues (target-to-background) is reduced and compromises the quality of MRA. Thus, as demonstrated in the current studies, conventional low-molecular-weight agents, such as Gd-DTPA, are not well suited for high-resolution MRA. Another important parameter that determines the quality of angiograms is the blood elimination rate of contrast agent. The conventional contrast agents are eliminated rapidly

from blood circulation through renal clearance. Although they do not penetrate the blood-spinal cord barrier, the rapid clearance of these contrast agents from blood circulation limits their use in acquiring angiograms with long scan times.

Liposomal-Gd has several advantages over conventional low-molecular-weight gadolinium chelates. The long intravascular half-life of liposomal-Gd allows for stable opacification of the blood vessels for the duration required for acquisition of high-resolution images. Furthermore, the microscopic size of these agents restricts their circulation to the vascular compartment, in regions of low capillary leak, and limits diffusion away from the vasculature in regions of high vascular permeability. The result of these 2 features is to limit the amount of enhancement of the extravascular tissues. Although the vascular signal intensities in the post–Gd-DTPA images were higher than in liposomal-Gd images, the CNRs obtained with liposomal-Gd were higher than those obtained with Gd-DTPA (Table 1). Rapid diffusion of Gd-DTPA into the extravascular compartment is probably responsible for the enhancement of the extravascular soft tissues that results in poor contrast between the vessels and the surrounding tissues. Acquiring high-resolution images with Gd-DTPA would therefore be expected to result in even more indistinct angiograms because of 1) significant extravascular diffusion during long scan times and 2) elimination from systemic circulation due to renal clearance.

The high-resolution angiograms obtained with liposomal-Gd demonstrated very good microvessel conspicuity (Fig 2). The PSV, ASA, and radicular arteries were clearly demonstrated in the MIP images (Fig 4). The intravascular nature of the liposomal-Gd agent also enabled visualization of the epidural venous plexus. The epidural venous plexus, which consists of a lattice of fine venules, has an amorphous appearance rather than discrete, because the diameters of these fine venules are much smaller than the voxel size of the image acquisition. The CNRs in the post–liposomal-Gd images were significantly higher than precontrast images (Table 2).

In addition to the liposomal-Gd agent, several other factors were critical in obtaining the high quality angiograms. A radio-frequency coil was surgically implanted within the soft tissues of the back of the animal and inductively coupled to an external surface coil. This enabled imaging with high SNR, which resulted in demonstration of several perispinal microvessels (Fig 4). A short echo time was used in the gradient-echo sequence to obtain a more heavily T1-weighted image. The repetition time was maintained as short as possible to reduce the overall scan time and thus allow for several signal intensity averages.

Although the current studies demonstrate vasculature external to the spinal cord with much detail, we have not been able to visualize the vessels within the spinal cord because of the resolution limitations and the low relaxivity of the liposomal-Gd agent. The ability to noninvasively visualize intraspinal cord vasculature would help greatly in defining the vascular lesions and microvascular reorganization in spinal cord injury.[22] It might also be possible to increase the image resolution by increasing the image matrix with concomitant increase in the scan time. However, this approach may be limited by morbidity and mortality associated with long anesthetic times. With the development of parallel imaging technology this limitation could be overcome to a great extent.[23]

The encapsulation of Gd-DTPA within the core of the liposomes results in limited water exchange across the lipid bilayer. The molar relaxivity of gadolinium encapsulated within liposomes is far lower than that observed in unencapsulated (free) Gd-DTPA. The encapsulation of Gd-DTPA inside these liposomes also alters the pharmacokinetics of Gd-DTPA. The clearance of liposomal-Gd occurs through the organs of reticuloendothelial system, namely liver and spleen, rather than the kidneys. Further in vivo studies should be done to investigate the possible concerns associated with the altered pharmacokinetics of the agent.

A unique characteristic of long-circulating liposomes is the ability to extravasate only from abnormal, leaky vessels. This property has been extensively exploited to deliver chemotherapeutic agents to solid tumors.[24] For grading and imaging solid tumors, the same characteristic of liposomal particles could therefore be used to overcome the confounding issues with conventional Gd-DTPA agent, which also leaks in normal microvasculature.[25] The encapsulation of gadolinium chelates within the liposomal interior also enables easy modification of the outer surface of the liposomes for actively targeting the contrast agents to specific sites (such as tumors, inflammation, injury, etc).

Conclusions

The liposomal-Gd enabled acquisition of angiograms with higher microvessel conspicuity than conventional Gd-DTPA because of the relative lack of extravascular enhancement that resulted in improved target-to-background contrast. In addition, the prolonged intravascular residence time of liposomal-Gd allowed for longer scans, thus facilitating high-resolution angiograms.

Acknowledgments

We acknowledge Dr. Shi-Jie Liu, Pallavi Ahobila-Vajjula, and Tessy Chacko for their help in animal handling and preparation. Financial support from N.I.H. grant #1 S10 RR17205 to P.A.N. is also acknowledged.

References

1. Loy DN, Crawford CH, Darnall JB, et al. **Temporal progression of angiogenesis and basal lamina deposition after contusive spinal cord injury in the adult rat.** *J Comp Neurol* 2002;445:308–24
2. Popovich PG, Horner PJ, Mullin BB, et al. **A quantitative spatial analysis of the blood-spinal cord barrier. I. Permeability changes after experimental spinal contusion injury.** *Exp Neurol* 1996;142:258–75
3. Nijenhuis RJ, Leiner T, Cornips EM, et al. **Spinal cord feeding arteries at MR angiography for thoracoscopic spinal surgery: feasibility study and implications for surgical approach.** *Radiology* 2004;233:541–47
4. Goyen M, Debatin JF. **Gadopentetate dimeglumine-enhanced three-dimensional MR-angiography: dosing, safety, and efficacy.** *J Magn Reson Imaging* 2004;19:261–73
5. Kobayashi H, Sato N, Hiraga A, et al. **3D-micro-MR angiography of mice using macromolecular MR contrast agents with polyamidoamine dendrimer core with reference to their pharmacokinetic properties.** *Magn Reson Med* 2001;45:454–60
6. Wang YX, Hussain SM, Krestin GP. **Superparamagnetic iron oxide contrast agents: physicochemical characteristics and applications in MR imaging.** *Eur Radiol* 2001;11:2319–31
7. Fiford RJ, Bilston LE. **The mechanical properties of rat spinal cord in vitro.** *J Biomech* 2005;38:1509–15
8. Falconer JC, Narayana PA, Bhattacharjee MB, et al. **Quantitative MRI of spinal cord injury in a rat model.** *Magn Reson Med* 1994;32:484–91

9. Young W. **Spinal cord contusion models.** *Prog Brain Res* 2002;137:231–55
10. Mantha A, Legnani FG, Bagley CA, et al. **A novel rat model for the study of intraosseous metastatic spine cancer.** *J Neurosurg Spine* 2005;2:303–07
11. Narayana PA. **Magnetic resonance of spinal cord injury.** In: Marwah J, Dixon E, Banik N, eds. *State-of-the-Art Handbook on CNS Trauma.* Scottsdale, Ariz: Prominent Press; 2001:137–178
12. Fenyes DA, Narayana PA. **In vivo diffusion tensor imaging of rat spinal cord with echo planar imaging.** *Magn Reson Med* 1999;42:300–06
13. Allen TM, Hansen C, Martin F, et al. **Liposomes containing synthetic lipid derivatives of poly(ethylene glycol) show prolonged circulation half-lives in vivo.** *Biochim Biophys Acta* 1991;1066:29–36
14. Ayyagari AL, Zhang X, Ghaghada KB, et al. **Long-circulating liposomal contrast agents for magnetic resonance imaging.** Magn Reson Med 2006;55:1023–29.
15. Mukundan S Jr., Ghaghada KB, Badea CT, et al. **A liposomal nanoscale contrast agent for preclinical CT in mice.** *AJR Am J Roentgenol* 2006;186:300–07
16. Bilgen M, Abbe R, Narayana PA. **Dynamic contrast-enhanced MRI of experimental spinal cord injury: in vivo serial studies.** *Magn Reson Med* 2001;45:614–22
17. Bilgen M, Elshafiey I, Narayana PA. **In vivo magnetic resonance microscopy of rat spinal cord at 7 T using implantable RF coils.** *Magn Reson Med* 2001;46:1250–53
18. Koyanagi I, Tator CH, Lea PJ. **Three-dimensional analysis of the vascular system in the rat spinal cord with scanning electron microscopy of vascular corrosion casts. Part 1: Normal spinal cord.** *Neurosurgery* 1993;33:277–83
19. Tveten L. **Spinal cord vascularity. II. Extraspinal sources of spinal cord arteries in the rat.** *Acta Radiol Diagn (Stockh)* 1976;17:167–79
20. Tveten L. **Spinal cord vascularity. IV. The spinal cord arteries in the rat**. *Acta Radiol Diagn (Stockh)* 1976;17:385–98
21. Bilgen M, Al-Hafez B, He YY, et al. **Magnetic resonance angiography of rat spinal cord at 9.4 T: a feasibility study.** *Magn Reson Med* 2005;53:1459–61
22. Schwartz ED. **MRI and the evaluation of blood-spinal cord barrier following injury.** *AJNR Am J Neuroradiol* 2005;26:1609–10
23. Pruessmann KP. **Parallel imaging at high field strength: synergies and joint potential.** *Top Magn Reson Imaging* 2004;15:237–44
24. Lasic DD, Martin, FJ. *Stealth liposomes.* Boca Raton, Fla: CRC Press; 1995
25. Brasch R, Turetschek K. **MRI characterization of tumors and grading angiogenesis using macromolecular contrast media: status report.** *Eur J Radiol* 2000;34:148–55